

# Anomalous electronic conductance in quasicrystals

Stephan Roche

\* *Department of Applied Physics, University of Tokyo, 7-3-1 Hongo, Bunkyo-ku, Tokyo 113-8654, Japan.*  
(October 23, 2018)

Contributions of quantum interference effects occurring in quasicrystals are reported. First conversely to metallic systems, quasiperiodic ones are shown to enclose original alterations of their conductive properties while downgrading long range order. Besides, origin of localization mechanism are outlined within the context of the metal-insulator transition (MIT) found in these materials.

PACS numbers: 72.90.+y 61.44.Br 72.10.-d

## I. INTRODUCTION

Despite sustained effort and concern, today's understanding of exotic electronic properties of quasicrystals<sup>1</sup> remains unsatisfactory although quasicrystalline materials have already been implemented to miscellaneous concrete applications<sup>2,3</sup>. In particular, the role of quasiperiodic order on electronic localization and transport is believed to genuinely entail the most unexpected experimental features whereas so far, no coherent theoretical framework has been really successfully ascertained<sup>4-7</sup>. As a matter of fact, one of the unprecedented tendency of quasicrystals is the enhancement of their conductive ability upon increasing contribution of static (structural disorder) or dynamical excitations (phonons). This has been strongly supported by many experimental evidences<sup>4</sup> and is often referred as an original property in the literature. Notwithstanding theoretically, given heuristical arguments<sup>5,8</sup> and numerical investigations (e.g. the Landauer conductance for quasiperiodic Penrose lattices<sup>9</sup> or Kubo formula for 3D-quasiperiodic models<sup>10</sup>) yield to uncomplete understanding of the observed properties which range from anomalously metallic behaviors to insulating ones<sup>7</sup>.

It is generally assumed that a specific "geometrical localization process" takes place in quasicrystals (sustained by critical states<sup>11,12</sup>) and that local disruptions of corresponding mesoscopic order reduce quantum interferences, resulting in an increase of conductivity. This issue has been tackled for 1D quasiperiodic potential, tight-binding (TBM) as well as continuous Kronig-Penney models, and phason-type disorder has been shown to disclose manifestations of quantum interferences (QIE) in quasiperiodic order<sup>15</sup>.

Pioneer works of M. Kohmoto<sup>11</sup> on multifractal properties of critical states in 1D-quasiperiodic chains have been recently followed by renewed focus on the relation between localization features of such states and their ability to convey current<sup>12</sup>. Still, variety of critical states let the question about localisation properties and transport ability relation unresolved. The effect of disorder on top of these states is thus a complicated issue and very scarce rigorous results are available in the literature. Attempts to rigorously establish analytical results in high-

dimensional quasiperiodic systems have been facing some limitations despite encouraging early attempts<sup>16,17</sup>.

In what follows, we review exact results carried out on 1D unperfected quasiperiodic systems. We also give additional and complementary results to enlarge the understanding of an early study<sup>15</sup>. Besides, the role of quantum interferences on both sides of the quasicrystalline MIT for higher dimensional materials is outlined in a second part. A general scenario to follow the metal-insulator is drawn in the light of recent results.

## II. INTERFERENCE EFFECTS IN 1D QUASIPERIODIC SYSTEMS WITH DISORDER

Introducing disorder could be done through typical randomizing of site or hopping energies, with the subsequent occurrence of Anderson localization in the infinite chain limit. For finite systems, localization lengths may be much larger than the characteristic size so that conductance fluctuations as a function of energy of tunneling electrons (from the leads to the system) keep its self-similar nature and still follow power law behavior for system size studied in<sup>13</sup> even when introducing disorder of 10% of the total bandwidth. However, the particular order sustaining long range quasiperiodicity suggest the possible presence of unique defects, known as phason-type defects. Their geometrical definition and properties have been subjected to many studies<sup>14</sup>, although some aspects remain controversial. From certain viewpoint it seems natural to consider how disruptions of quasiperiodic order inherent to such systems will degrade or improve transport properties. It is the aim of this work to contribute to such more general and fundamental understanding of electronic propagation in quasicrystals.

For 1D-quasiperiodic systems, we can define phasons that keep the essential characteristic of real systems, in the sense that they are a generic form of disorder which has no equivalent in usual metallic and periodic systems. In a preliminary study, such phason defects were introduced by K. Mouloupoulos, as a main probe for investigating Landauer conductance<sup>15</sup>.

Tight-binding models (TBM) of perfect quasiperiodic chains have been intensively worked out both analytically



where  $t(N)$  are integers and  $s(N)$  are described by a recursive relation. For the Fibonacci sequence  $N = \{F_1, F_2, \dots, F_{N-1}, F_N\}$ , H. Kubo and M. Goda<sup>20</sup> have investigated the statistical properties of  $s(N)$  which are directly related to the characteristic exponents of self-similar wavefunctions. Taking  $(\psi_0, \psi_{-1}) = (-i, 1)$ , it is possible to show that  $|\psi_n|^2 = \gamma^{-2s(N) \times (-1)^{t(N)}}$ . The Landauer resistance of a finite chain  $N$  is given by  $\rho_N = \frac{h}{e^2} \frac{R}{T}$  where  $T$  is the fraction of tunneling electrons transmitted from the system to the leads, and  $R$  is the reflected one. For a tight-binding model one relates the resistance to the total transfer matrix elements:  $\rho_N = \frac{1}{4}(P_N^2(1, 1) + P_N^2(1, 2) + P_N^2(2, 1) + P_N^2(2, 2) - 2)$ .

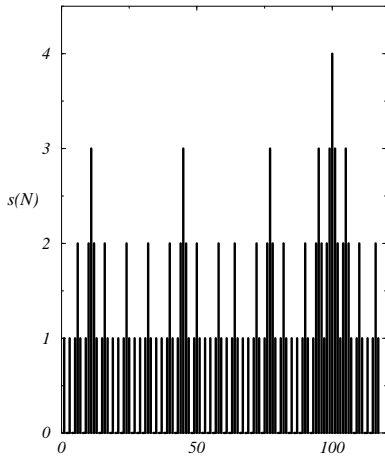


FIG. 2. Multifractal distribution of  $|s(N)|$  for the Fibonacci chain of 800 sites.

and one write the Fibonacci chain's resistance in a closed form

$$(\rho_N)_I = \frac{1}{4}(\gamma^{2s(N)} + \gamma^{-2s(N)}) - \frac{1}{2} = \left( \frac{\gamma^{s(N)} - \gamma^{-s(N)}}{2} \right)^2$$

The function  $s(N)$  is illustrated on Fig. which manifest self-similar pattern. When  $s(N_0) = 0$ , transmission is perfect  $T = 1$ . If one considers the Lyapunov exponents for finite length systems we get some estimates of the associated localization lengths at a given energy<sup>22</sup>. By definition effective Lyapunov exponents (since localization length can be much larger than system size in the finite limit) for a chain of  $N$  sites are given by  $\rho_N(E) = \frac{h}{2e^2} \exp(\gamma_N(E) \times N)$  which is equivalent to  $\gamma_N(E) = \frac{1}{N} |P_N(1, 2)|^2$  (given that  $\rho_N(E) = |P_N(1, 2)|^2$ ).

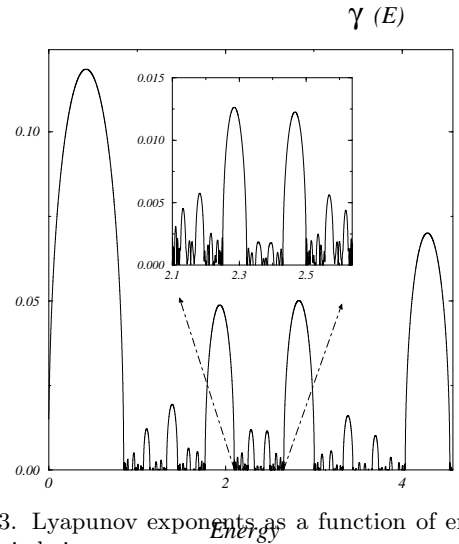


FIG. 3. Lyapunov exponents as a function of energy of a Fibonacci chain.

For energies lying outside the spectrum are easily identified with stronger Lyapunov exponent as exemplified on Fig.. The cantor spectrum for eigenvalues is revealed by the corresponding self-similar pattern of localization lengths distribution.

We now remind the effect of phason defect on the Landauer resistance obtained in<sup>15</sup>. Taking the position of the defect, represented by a  $-BB-$  unit as an internal degree of freedom, at  $E=0$ , the properties of the matrices  $\mathcal{A}, \mathcal{B}, \mathcal{C}$  are shown to be independent of the position henceforth called  $x_P$ <sup>15</sup>. By simple manipulations of the transfer matrix, we further demonstrate that the total transfer matrix associated to the chain with one phason and with  $N(i)$  links is the same as the one without phason but with  $N(i+2)$  links. Accordingly, a generic form can be written down :  $P_N$  (with either  $a = d = 0$ , or  $b = c = 0$ )

$$P_{N(i)}|_I = \begin{pmatrix} a & b \\ c & d \end{pmatrix} \quad (5)$$

then

$$P_{N(i)}|_{III} = P_{N(i+2)}|_I = - \begin{pmatrix} 0 & -\gamma \\ 1 & 0 \end{pmatrix} \begin{pmatrix} 0 & -\frac{1}{\gamma} \\ 1 & 0 \end{pmatrix} \begin{pmatrix} a & b \\ c & d \end{pmatrix} \quad (6)$$

Landauer resistance was shown to be given by<sup>15</sup>:

$$(\rho_N)_{III} = \left( \frac{\gamma^{s(N)-1} - \gamma^{-s(N)+1}}{2} \right)^2$$

By comparing the two expressions for the Landauer resistance one concludes that at  $E = 0$ , the sign of  $\rho_N|_I - (\rho_N)_{III}$  is fluctuating as a function of chain-length, which means the phason defect does not alter the transport properties in the infinite limit.

We now consider the sequence constructed following the same algorithm but maximizing the number of phason defects as identified by **BB**. We then calculated analytically the Landauer resistance  $\rho_N|_{IV}$ . For instance for chains with  $N=4$  and  $N=17$  links, one has :

$$\begin{aligned} & (B) - ABBA - (B) \\ & (B) - ABBABBAABABBABBA - (B) \end{aligned}$$

With the same transfer matrices previously introduced  $\mathcal{A}, \mathcal{B}$  and noticing that  $BAABAB$  and  $BAB$  are equal respectively to  $\mathcal{A}$  and  $-\mathcal{B} = \tilde{\mathcal{B}}$ , we show that the sequence of  $P_N|_{IV}$  is generated by the following Fibonacci sequence  $P_N = \mathcal{A}, \mathcal{A}\tilde{\mathcal{B}}, \mathcal{A}\tilde{\mathcal{B}}\mathcal{A}, \mathcal{A}\tilde{\mathcal{B}}\mathcal{A}\mathcal{A}\tilde{\mathcal{B}}, \mathcal{A}\tilde{\mathcal{B}}\mathcal{A}\mathcal{A}\tilde{\mathcal{B}}\mathcal{A}\tilde{\mathcal{B}}, \mathcal{A}\tilde{\mathcal{B}}\mathcal{A}\mathcal{A}\tilde{\mathcal{B}}\mathcal{A}\tilde{\mathcal{B}}\mathcal{A}\mathcal{A}\tilde{\mathcal{B}}, \dots$ . The analytical form of  $\rho_N|_{IV}$  is shown to be given by

$$(\rho_N)_{IV} = \left( \frac{\gamma^{\tilde{s}(N)} - \gamma^{-\tilde{s}(N)}}{2} \right)^2$$

with  $\tilde{s}(N)$  a new complex function of  $N$  calculated iteratively. The interesting point to observe is that the function  $\rho_N|_I - \rho_N|_{III}$  for one phason defect changes its sign at each step  $N \rightarrow N+1$ , whereas  $\rho_N|_I - \rho_N|_{IV}$  manifestes fluctuations on much larger range. As an illustration, chains with number of sites respectively equal to  $N(i = 1, 2, 3, 4, 5 \dots 17) = 5 - 203$  sites follow  $\rho_N|_I - \rho_N|_{IV} \geq 0$ , whereas the behavior is opposite for chain from 330 to 456 sites, and so forth.

In conclusion, even for the highest density, such phason disruptions of quasiperiodic order are not able to break down the localization mechanism which do remain basically the same in the limit  $N \rightarrow \infty$ .

### III. LANDAUER RESISTANCE OF A KRÖNIG PENNEY MODEL WITH PHASONS

Hereafter we first rewrite the main steps of calculations as first described in<sup>15</sup>. We then perform power-spectra calculations of Landauer resistance interference patterns to clarify the differences between localization properties and transmission abilities of critical states. In the Krönig

Penney model<sup>23</sup>, the potential describing the interaction of the electron with the lattice is represented by a sum of Dirac distributions with intensity  $V_n$  localized at  $x_n$   $V(x) = \sum_n V_n \delta(x - x_n)$ , the  $x_n, V_n$  can be chosen as correlated variables, or uncorrelated. In between two successive scattering centers, the solution of the Schrödinger equation is a linear combination of two plane waves:  $\Psi(x) = A_n e^{ik(x-x_n)} + B_n e^{-ik(x-x_n)}$  ( $x_n \leq x \leq x_{n+1}$ ), the 1D wavevector  $k > 0$  is related to the energy  $E$  through  $E = \hbar^2 k^2 / 2m$ . In the Krönig-Penney (KP)<sup>23</sup> model, a solution of the problem is constructed by imposing continuity conditions for the wavefunction and its derivative. For sake of simplicity, we choose the case where the intensity of scattering potential is constant  $=\lambda$ , whereas scattering centers are quasiperiodically spaced  $\{(x_n - x_{n-1})\} = \{a, b\} = \{\tau, 1\}$ . The problem can then be written as followed :

$$\begin{pmatrix} A_{n+1} \\ B_{n+1} \end{pmatrix} = \Lambda(n) \cdot \begin{pmatrix} A_n \\ B_n \end{pmatrix} \quad (7)$$

with

$$\Lambda(n) = \begin{pmatrix} (1 - \frac{i\lambda}{2k})e^{ik(x_{n+1}-x_n)} & -\frac{i\lambda}{2k}e^{ik(x_{n+1}-x_n)} \\ \frac{i\lambda}{2k}e^{-ik(x_{n+1}-x_n)} & (1 + \frac{i\lambda}{2k})e^{-ik(x_{n+1}-x_n)} \end{pmatrix} \quad (8)$$

within this framework, Landauer resistance is given by  $\rho_N = |P_n(1, 2)|^2$  with  $P_n = \Lambda(F_n) \dots \Lambda(1)$ . Furthermore, a renormalization group associated with the Fibonacci chain enables to map the electronic spectrum to a dynamical system associated with the traces of the transfer matrices. The following energy-dependent invariant of the Krönig-Penney model is convenient to consider<sup>24</sup>. In our case, we find  $I(k) = \frac{\lambda^2 \sin^2 k(a-b)}{4k^2}$  whose zeros are given by  $k_s = n\pi/(a-b)$ , with  $n$  integer. These points referred as conducting points are interesting since they correspond to the commutation of the transfer matrices,  $[P_{F_n}, P_{F_{n+1}}] = 0$  given that  $4I + 2 = \text{Tr}(P_{F_n} \cdot P_{F_{n+1}} \cdot P_{F_n}^{-1} \cdot P_{F_{n+1}}^{-1})$ . Besides elementary matrices also commute :

$$[\Lambda(\Delta x = a), \Lambda(\Delta x = b)] = \lambda \frac{e^{ik(a-b)}}{4k^2} (1 - e^{2ik(b-a)}) \begin{pmatrix} \lambda & \lambda - 2ik \\ -\lambda - 2ik & -\lambda \end{pmatrix} \quad (9)$$

The resistance can be written down analytically at  $k_s$

$$\rho_N|_{k=k_s} = \left( \frac{\lambda}{2k_s} \right)^2 \frac{\sin^2 N\varphi}{\sin^2 \varphi} \quad (10)$$

with  $\varphi$ , depending on  $k_s^2$  and  $\lambda$ , and is defined equivalently by  $\cos \varphi = \cos k_s a + \lambda / 2k_s \sin k_s a$  or  $\cos \varphi =$

$\cos k_s b + \lambda / 2k_s \sin k_s b$ . The analytical form of  $\rho_N|_{k=k_s}$  indicates that when  $N \rightarrow \infty$ , the Landauer resistance oscillates but remains bounded, so that the energies  $k_s^2$  correspond to states that lead to best transmission, reminding that localized states will display exponential increase of resistance. Following the discussion of<sup>18,19</sup>, if ones re-

stricts the study for energies  $k^2 = (k_s + \varepsilon)^2$  in the vicinity of  $k_s$  where highest density of eigenvalues are expected in the infinite limit (hereafter  $k_s = \pi/(\tau - 1)$ , ( $a = \tau$ ,  $b = 1$ ))

$$\Lambda_A = \begin{pmatrix} (1 - \frac{i\lambda}{2k})e^{ik\tau} & -\frac{i\lambda}{2k}e^{ik\tau} \\ \frac{i\lambda}{2k}e^{-ik\tau} & (1 + \frac{i\lambda}{2k})e^{-ik\tau} \end{pmatrix}$$

Choosing  $\lambda$  so that  $\rho_N|_{k=k_s} = 0$  exactly at  $k = k_s$ , which lead to  $N - 1$  values for  $\lambda$ , given by  $\lambda_s = \frac{2k_s(\cos \varphi_s - \cos k_s)}{\sin k_s}$  with the phase  $\varphi_s$  defined through  $\varphi_s = (m\pi)/N$  with  $m=1, \dots, N-1$ . The  $N-1$  values  $\varphi_s$  are symmetrically distributed around  $\pi/2$  and cover densely the half-upper trigonometric plane when increasing  $N$ <sup>15</sup>. Reminding that  $x_P$  is taken as the position of phason defect (**BB**) in the chain, with  $x_P \in [1, P]$  an integer and  $P$  the maximum number of position for a given chain, we know recall main important patterns<sup>15</sup> and perform power spectra of  $\rho_N(x_P, \varphi_s, \varepsilon)$ .

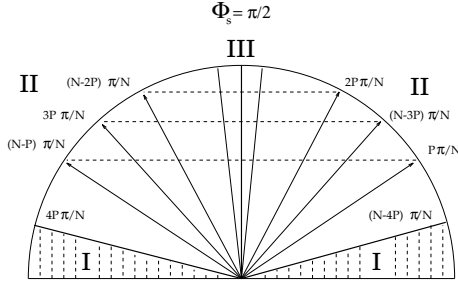


FIG. 4. Energy dependent phase diagram.

Numerical accuracy is checked through  $P_N(1, 1)^2 - 1 = P_N(1, 2)^2$  which gives the resolution. The Landauer resistance calculated in  $k = k_s$  is always found to be  $\sim 10^{-12} - 10^{-13}$  and gives thus the numerical uncertainty on  $\rho_N$ . We now present the main results as sketched on the phase diagram in Fig.. According to the variable  $\varphi_s$  ones identifies several features. First, note that amazing pseudo-symmetry is found around  $\pi/2$  for  $\rho_N(x_P, m, \varepsilon)$

is taken without loss of generality). Two transfer matrices are defined

$$\Lambda_B = \begin{pmatrix} (1 - \frac{i\lambda}{2k})e^{ik} & -\frac{i\lambda}{2k}e^{ik} \\ \frac{i\lambda}{2k}e^{-ik} & (1 + \frac{i\lambda}{2k})e^{-ik} \end{pmatrix} \quad (11)$$

which do not correspond to any symmetry in the scattering potential (see below Fig.- for illustration).

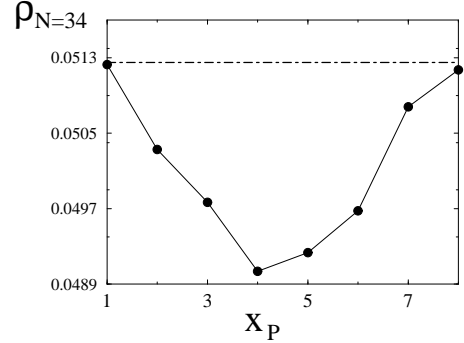


FIG. 5. Landauer resistance as a function of phason position  $x_P$ , for  $\varepsilon = 10^{-4}$ ,  $N = 35$  sites and  $m=1$ .

In the zones referred as zone-I the phason reduces the resistance for energies sufficiently close to the conducting points (see Fig.-). Two symmetrical zones are  $m < N - 4P$ , and  $m > 4P$  with  $\rho_N |_{\text{I}}(x_P, m, \varepsilon) > \rho_N |_{\text{III}}(x_P, m, \varepsilon)$ . In other words, for that values of parameters the Fibonacci chain becomes more conductive upon introduction of local phason. This effect is a pure result of quantum interference at low temperature and has been shown for tunneling energies close to the ones of conducting points, so for the electrons that can better contribute to conduction mechanism. We illustrate these behaviors first on Fig. which allow to write down all the 8 different inequivalent defected-chains as described below for clarity for a system with 35 sites:

*FIBO* : -- B -- ABAABABAABAABABAABAABAABAABAABAAB -- B --  
*Def1* : -- B -- A**BB**ABAABAABAABAABAABAABAABAABAABAAB -- B --  
*Def2* : -- B -- ABAABABA**BB**AABAABAABAABAABAABAABAABAAB -- B --  
*Def3* : -- B -- ABAABABAABA**BB**AABAABAABAABAABAABAABAAB -- B --  
*Def4* : -- B -- ABAABABAABAABA**BB**AABAABAABAABAABAABAAB -- B --  
*Def5* : -- B -- ABAABABAABAABAABA**BB**AABAABAABAABAABAAB -- B --  
*Def6* : -- B -- ABAABABAABAABAABAABA**BB**AABAABAABAABAAB -- B --  
*Def7* : -- B -- ABAABABAABAABAABAABAABA**BB**AABAABAABAAB -- B --  
*Def8* : -- B -- ABAABABAABAABAABAABAABAABA**BB**ABA -- B --

Besides, the function  $\rho_N |_{\text{III}}(k, m, x_P)$  given a kind of interference pattern by the position of phason defect described by the position of phason defect  $\rho_N |_{\text{III}}(k, m, x_P) \sim \alpha(m/P) \sin(\frac{2m\pi}{P}x_P)$ . This is further represented on Fig. for chains with  $N=2000$  links, and  $m=1,5$ . The curves for  $m=1$  (Fig. and Fig.(top)) and different chain lengths shows that the interference pattern encloses a memory of self-similarity.

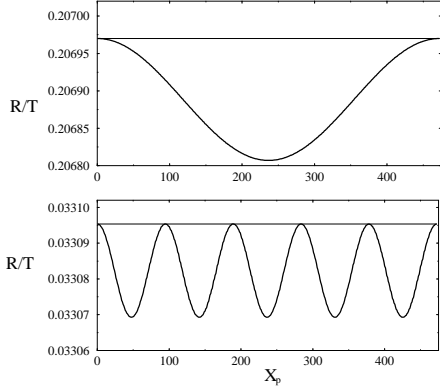


FIG. 6. Landauer resistances as a function of phason position  $x_P$  ( $N=2001, P=472$ ) for  $\varepsilon = [10^{-9}, 10^{-6}]$  and  $m=5$ . For higher values of  $\varepsilon$ , then  $\rho_N \rightarrow \infty$  which indicates that energy lies within a gap, or may be associated with a localized state.

The power spectrum of  $m=5$  curve is given on Fig., where the only eigenfrequency agrees with  $m/P = 5/472 = 0.0106$  in this case. Superimposed small oscillations are an unphysical effect due to a Fourier transform of a finite signal.

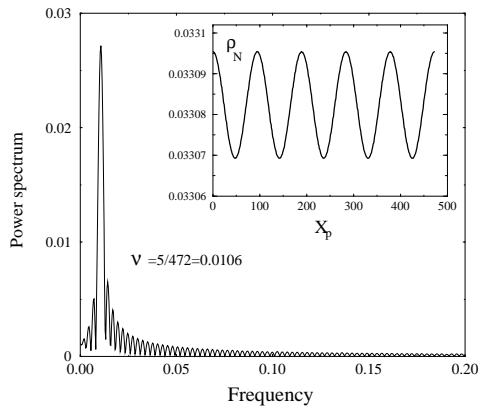


FIG. 7. Power spectrum of the pattern given in the inset for  $m=5$  and same parameters as previous figure (bottom).

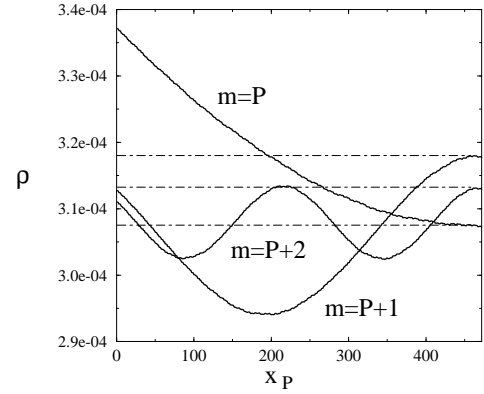


FIG. 8. Regular evolution of interference pattern for  $m = P, P+1, P+2$  and  $N = 2000, P = 472$ . For  $\varphi_s = P\pi/N$ , Fibonacci chain is always less resistive than the imperfected one whereas transition occurs for  $m = P+1, P+2, \dots$  dashed curves are the values for Fibonacci chains with same parameter  $m$  as imperfected one.

Let's move forward to zone-**II**. for  $N - 4P < m < 4P$  situations become more complex but recurrent simple  $(m - P)$ -periodic oscillatory patterns are found around the values  $\varphi_s = \{(N - 4P)/N, (N - 3P)/N, (N - 2P)/N, (N - P)/N\} \pi$  and symmetrically for  $\tilde{\varphi}_s = \{4P/N, 3P/N, 2P/N, P/N\} \pi$ . In these regions of parameter space, there is a genuine transition from systematic increasing to decreasing (and vice versa) of the electronic resistance upon introduction of phason, as exemplified on Fig..

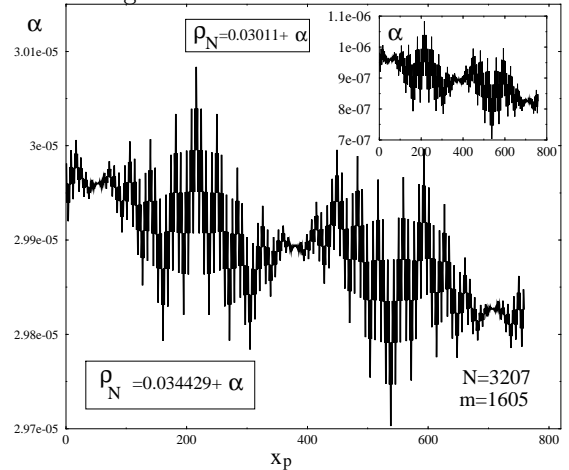


FIG. 9. Landauer resistance for values of scattering potential which unravel self-similar patterns as described in the text.

As far as zone-**III** is concerned, and related to some interval around  $\varphi \sim \frac{\pi}{2}$ , self-similar patterns are observed which suggest that  $\rho_N |_{\text{III}}(x_P)$  reveal critical states which are robust against phason disorder as found in the TBM for  $E=0$  case. The typical patterns represented on Fig. actually enclose oscillations of resistance which smaller oscillations are described by some coefficients  $s(n)$  as described previously.

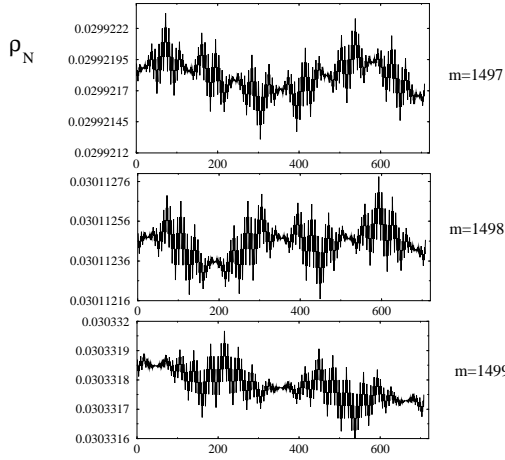


FIG. 10. Interferences pattern for several values of scattering potentials close to  $\varphi \sim \frac{\pi}{2}$ .

On the Fig., the case with 3000 sites is considered and different values of the scattering potential in the vicinity of the symmetry point  $\varphi = \frac{\pi}{2}$ . For  $m=1497$ , the potential is  $\lambda \sim 3.918$ , for  $m=1498$   $\lambda \sim 3.929$  and  $3.941$  for  $m=1499$ . Patterns exhibit small differences, and their Fourier spectrum is actually very similar (see below).

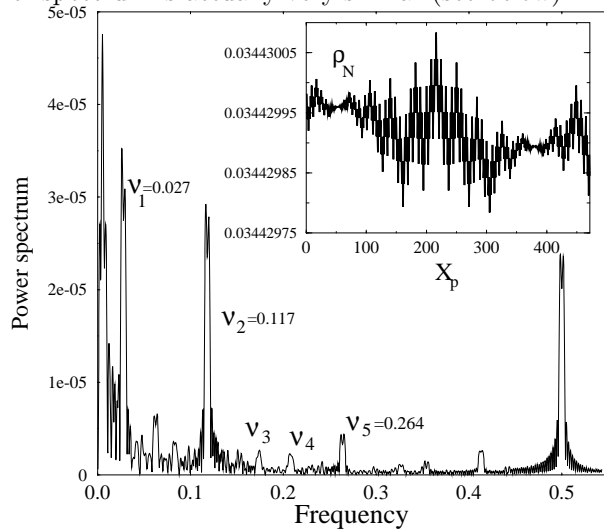


FIG. 11. Self similar interference pattern for  $N=3207$ ,  $P=757$  and  $J=1605$ . Stability is ensured from  $\varepsilon = 10^{-3}$  down to the numerical resolution limit.

The power spectra of different similar patterns are given on Fig. and Fig. which show that superimposed frequencies are identical. The highest frequency is given by  $\nu = 0.5$  which is related to the change of  $\rho_N(x_P \rightarrow x_P + 1)$ . On respective figures five unambiguous frequencies have been located and named  $\nu_{n=1,5}$ . This prove that all these self-similar patterns are actually described by exactly the same function which is a superposition of several independent frequencies convolute with a function defined by a serie of  $s(N)$ -type coefficients. Concerning all the discussed zones-**I**, **II**, **III**, simple forms for energies sufficiently close to conducting points. Then  $\rho_N(x_P, \varepsilon)$  result from a superposition of one or several frequencies. For

larger energies one finds fluctuations as those analyzed in the inset of Fig.. As energies get farther to conducting points  $k_s = \pi/(\tau - 1)$  the resistance is sharply increasing on several order of magnitudes. The power spectrum in this case reveal much more eigenfrequencies, with the interesting emergence of frequencies with similar amplitudes referred as  $\nu$  and  $\omega$ . In all these cases the respective behaviors of the Landauer resistance of the perfect Fibonacci chain versus the imperfect one follows complicated random fluctuations.

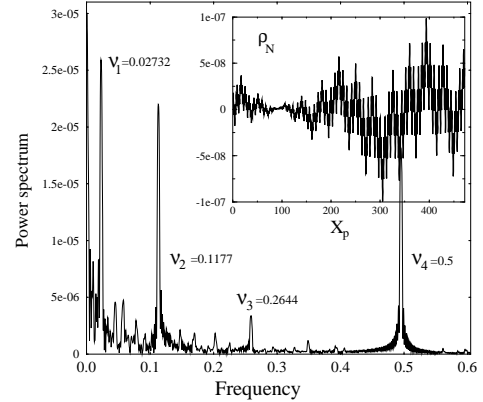


FIG. 12. Same as previous figure with different  $m$ .

The different behaviors found in these studies suggest that in some case local disruption of long range quasiperiodic order has improved the conductive ability of the chain in a systematic manner. Analyzing the interference pattern of the Landauer resistance as a function of phason defect suggest that extendedness (as a localization properties of available states at such energies) has also been jointly improved. This is shown by a bounded and simple oscillatory pattern for the resistance, common to what is found for extended eigenstates in a periodic systems.

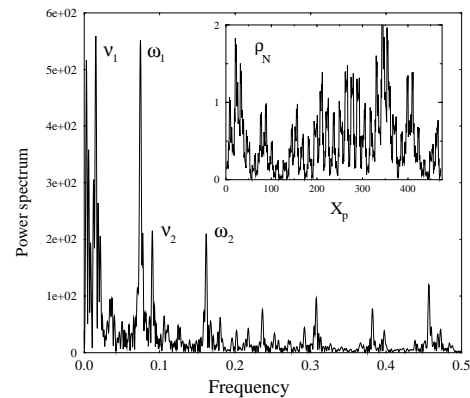


FIG. 13. Landauer resistance interference pattern for  $\varepsilon = 0.5$ ,  $N=2000$  and  $P=472$ .

To conclude this study, one stresses that first conducting points indeed seem to be the location of high density of eigenenergies as discussed in<sup>18,19</sup> and Krönig Pen-

ney model has been able to unravel specific quantum interference effects of phason disorder on localization and propagation properties, hidden in the treatment of TBM, and appealing in the context of quasicrystalline materials. Here following earlier results<sup>15</sup>, we have found that multi phason defects in TBM at E=0, do not alter the transmission abilities of corresponding states, and that interference patterns as revealed by  $\rho_N(x_P, \varepsilon)$  and their power-spectra analysis is an original way discovering how phason defects affect jointly localization and transport modes.

#### IV. QUANTUM INTERFERENCE MECHANISMS IN HIGH-DIMENSIONAL QUASICRYSTALS

Some effort to investigate quantum interferences effects in small quasiperiodic penrose approximants have been made<sup>16</sup>. Here we propose how quantum interferences on both sides of a metal-insulator transition in real materials might be analyzed. Indeed, weak localization regime has been found in experiments for some quasicrystalline materials (AlCuFe, ...) whereas other systems such as AlPdRe-quasicrystals behave differently being very close to a metal-insulator transition<sup>4</sup>. Two different focus may be considered for a general understanding of quantum interferences in quasicrystals. First, as there exist approximant phases (periodic) sharing the same behavior, weak localization correction beyond Drude approximation should apply for that systems as well as for corresponding quasicrystals. The only recurrent approximation when solving the cooperon diffusion equation is to assume that scatters are uncorrelated i.e  $\langle \mathcal{U}(r)\mathcal{U}(r') \rangle_{disorder} = cu^2\delta(r-r')$  ( $\mathcal{U}(r) = \sum_{i=1}^N \mathcal{U}(r-R_i)$ , c the impurity concentration, u typical strength). The calculation of the quantum correction of the conductivity in this regime is enclosed in phase factor interferences of the two-particle Green's function  $\langle GG^* \rangle$ . By performing configuration averaging beyond the mean free path length scale, then  $\langle GG^* \rangle_{disorder}$  reduces phase interference to the  $(k' = -k)$ -Cooperon pole, as a consequence of time reversal symmetry, the possibility to have a coherent distribution of scatters is usually neglected.

However, assuming that the distribution of scatters is constrained to, let's say for sake of illustration, a mirror-plane symmetry, i.e  $\forall \alpha \in \{R_\alpha, \alpha = 1, N\}$  there is a site  $R_\beta$  such that  $R_\beta = -R_\alpha$ , then without performing any diagrammatic expansion, we just notice that weak localization related with average of the potential scattering  $\langle \mathcal{U}(r)\mathcal{U}(r') \rangle_{disorder}$  corresponding to phase factors

$$\sum_{\alpha\beta} \langle e^{-i(k \cdot R_\alpha + p \cdot R_\beta)} \rangle_{disorder} = \frac{1}{\Omega^2} \int d^3R_\alpha d^3R_\beta e^{-ikR_\alpha} e^{-ipR_\beta}$$

will display new terms associated to above-mentioned symmetry,  $\langle e^{-i(k \cdot R_\alpha + p \cdot R_\beta)} \rangle_{disorder} =$

$\langle e^{i(p-k)R_\alpha} \rangle_{disorder} = \delta_{p-k,0}$  that will increase the contribution of phase interferences. Say in another way, if a double symmetrical loop crosses in the mirror plane and in a region with extension less or equal to  $\lambda_F$ , then four equivalent paths will interfere at the returning point instead of the usual two of the weak localization scheme, resulting in a total interference amplitude will be 4 times stronger ( $|\mathcal{A}_I + \mathcal{A}_{II} + \mathcal{A}_{III} + \mathcal{A}_{IV}|^2 = 16 |\mathcal{A}|^2$ ). Similar ideas have been already introduced in context of mesoscopic physics<sup>29</sup> but we propose here that they may serve as a path to follow a metal-insulator in quasicrystals in which even disorder (such as phasons) may keep some strong correlated properties<sup>25</sup>.

The second focus is suggested by the close proximity of a metal-insulator transition and gives a very dissimilar weight to quantum interferences. Any critical point of an electronic localisation-delocalisation transition can essentially be described by its anomalous diffusion which means that two-particle Green function reads  $\langle |G^+(r, r'; E)|^2 \rangle \sim |r-r'|^{-\eta+2-D}$  with  $\eta$  a critical exponent (and the propagator represents the transition probability in real space of an electron of E energy from site  $|r\rangle$  to  $|r'\rangle$ ), and which directly affect the conductivity of the system since

$$\sigma_{DC} = \frac{2e^2}{h} \lim_{\varepsilon \rightarrow 0} 4\varepsilon \int d^D r r^2 \langle |G^+(r, r'; E)|^2 \rangle_{disorder} \quad (12)$$

In the case where all states are localized (insulating side), the average is carried out over random configurations of frozen disorder and given that  $\langle |G^+(r, r'; E)|^2 \rangle_{imp} \sim \exp^{-|r-r'|/\xi_E}$  ones easily recovers that  $\sigma_{DC} \rightarrow 0$  at zero temperature. At the critical point, the power law describing electronic propagation has been illustrated in quantum Hall regime (D=2) for length scales in the regime of multifractality, i.e  $l \ll r \ll \xi$ ,  $\eta \simeq 0.38 \pm 0.04$ <sup>28</sup> or analytically in hierarchical potential<sup>26</sup> and quasiperiodic systems<sup>27</sup> and numerically in 3D quasiperiodic systems<sup>5,10</sup>. No characteristic length scales, such as the mean free path, can be defined and interference effects are intrinsically defining the dominant transport mechanism. A simple analysis of the equation 12 shows that according to the strength of criticality, as manifested by the value of the exponent, conductivity can be zero or infinite at zero temperature for a perfect system. Elastic scattering allow to work out the exponents of the anomalous Drude formula<sup>27,10</sup> at very low temperature.

At finite temperature, a dissipation mechanism results in a cut-off in the integral, and one always gets a finite value for the resistance. Since the interesting point occurs when multifractality dominate the transport regime, it is then important to estimate temperature dependent transport. In quasicrystals, critical states ( $\sigma \sim \tau^{2\beta-1}$ )<sup>5,27</sup>, where  $\tau$  is supposed to be the relevant inelastic scattering rates at a given temperature. From a scaling analysis of the Kubo formula on periodic quasicrystalline approximants, and from the knowl-

edge of exact eigenstates a scaling behavior was revealed  $\Delta\sigma(T) \sim T^\eta$ , with  $\eta \simeq 1.25$  in good agreement with the values obtained experimentally for several quasicrystalline and approximant phases at temperature  $\geq 10K^{30-32}$ .

In both side of the metal-insulator transition, the presence of phasons as demonstrated in 1D systems may weaken the interference effects while destroying quasiperiodic long range order, resulting thus in a unconventional mechanism. Working this out analytically in realistic models remains a great challenge.

## V. CONCLUSION

Several features occurring in the electronic transport of 1D quasicrystals have been reviewed. Quantum interferences have been shown to be interestingly altered by phason defects which may be a natural disruption of quasicrystalline disorder. In quasicrystals QIE may be sustained by different mechanisms as discussed in the second part. Revealed pattern in 1D-systems may keep some generality in higher dimension.

## ACKNOWLEDGMENTS

S.R. is indebted to the European Commission for financial support (Contract ERBIC17CT980059), and to Prof. T. Fujiwara from Department of Applied Physics of Tokyo University for hospitality. Kostas Mouloupoulos is deeply acknowledged for many enlightening discussions and encouragements.

---

<sup>1</sup> D. Shechtman, I. Blech, D. Gratias et J.W. Cahn, *Phys. Rev. Lett.* **51**, 1951 (1984).

<sup>2</sup> J.M. Dubois et al. *Annales de Chimie* **19**, 3 (1994). S. Roche, *Annales de Chimie* **23**, 953 (1998). E. Maciá, in *Revista Española de Física* (may 1998).

<sup>3</sup> *New Horizons in Quasicrystals: Research and Applications*, ed. A.I. Goldman, D.J. Sordelet, P.A. Thiel and J.M. Dubois, (World Scientific Singapore, 1997).

<sup>4</sup> C. Berger, *Seminar 3*, E. Akkermans, G. Montambaux, J.L. Pichard and J. Zinn-Justin eds. *Les Houches, Session LXI, Mesoscopic Quantum Physics* (1994).

<sup>5</sup> S. Roche, G. Trambly de Laissardière and D. Mayou, *J. of Math. Phys.* **38**, 1794 (1997).

<sup>6</sup> T. Fujiwara, in *Physical Properties of Quasicrystals*, Springer Series in Solid-State Sciences **126**, Editor Z.M. Stadnik, 169 (1999)

<sup>7</sup> S. Roche and T. Fujiwara, *Phys. Rev. B* **58**, 11338 (1998).

<sup>8</sup> C. Sire in "Lectures on Quasicrystals", ed. F. Hippert and D. Gratias (Les Editions de Physique Les Ulis, 1994).

<sup>9</sup> S. Yamamoto and T. Fujiwara, *Phys. Rev. B* **51**, 8841 (1995).

<sup>10</sup> S. Roche and D. Mayou, *Phys. Rev. Lett.* **79**, 2518 (1997).

<sup>11</sup> M. Kohmoto, L. P. Kadanoff, and Ch. Tang, *Phys. Rev. Lett.* **50** 1870 (1983); *ibid.* **50** 1873 (1983). M. Kohmoto, *Intern. J. of Mod. Phys. B* **1** 31 (1986). M. Kohmoto and J. R. Banavar, *Phys. Rev. B* **34** 563 (1986).

<sup>12</sup> E. Maciá and F. Domínguez-Adame, *Phys. Rev. Lett.* **76**, 2957 (1996). and references therein.

<sup>13</sup> S. Das Sarma and X.C. Xie, *Phys. Rev. B* **37**, 1097 (1988).

<sup>14</sup> T.C. Lubensky, J.E.S. Socolar, P.J. Steinhardt, P.A. Bancel and P.A. Heiney, *Phys. Rev. Lett.* **57**, 1440 (1986). G. Coddens, R. Bellissent, Y. Calvayrac, J.P. Ambroise, *Europhys. Lett.* **16** 271 (1991). A. Trub and H.R. Trebin, *J. Phys. France* **4** 1855-1866 (1994). H. Klein, M. Audier, M. Boudarda and M. de Boissieu, L. Behara and D. Duneau, *Phil. Magazine A* **73**, 309-331 (1996).

<sup>15</sup> K. Mouloupoulos and S. Roche, *Phys. Rev. B* **53**, 212 (1996).

<sup>16</sup> K. Mouloupoulos and S. Roche, *Journal of Condensed Matter C*: **7** 8883 (1995).

<sup>17</sup> K. Mouloupoulos, unpublished.

<sup>18</sup> J. Kollar and A. Süto, *Physics Letters A* **117**, 203 (1986).

<sup>19</sup> M. Baake, D. Joseph and P. Kramer, *Phys. Lett. A* **168**, 203 (1986).

<sup>20</sup> M. Goda and H. Kubo, *J. Phys. Soc. Jpn.* **58** 3624 (1989) ; H. Kubo and M. Goda, *J. Phys. Soc. Jpn.* **60** 2729 (1991) ; *J. Phys. Soc. Jpn.* **62** 2601 (1993).

<sup>21</sup> F. Wijnands, *J. Phys. A* **22**, 3267 (1989).

<sup>22</sup> A. Süto, in *Beyond quasicrystals*, edited by F. Axel and D. Gratias (Les Editions de Physique, France, 1994) 483.

<sup>23</sup> R. de L. Krönig and W.G. Penney, in *Mathematical Physics in One Dimension*, eds. E.H. Lieb and D.C. Mattis, p. 243.

<sup>24</sup> M. Baake, U. Grimm and D. Joseph, *Int. Journ. of Moder. Phys. B*, **7** Nos. 6&7 (1993) 1527.

<sup>25</sup> S. Roche, unpublished.

<sup>26</sup> G. Jona-Lasinio, F. Martinelli and E. Scoppola, *J. Phys. A: Math. Gen.*, **17** (1984) L635; *ibid Ann. Inst. Henri Poincaré* **42** (1985) 73.

<sup>27</sup> H. Schulz-Baldes and J. Bellissard, *Rev. Math. Phys.*, **10** 1 (1998). H. Schulz-Baldes, *Phys. Rev. Lett.* **78** , 2176 (1997).

<sup>28</sup> M. Janssen, *Intern. Journ. of Mod. Phys. B* **8**, 943 (1994).

<sup>29</sup> M. B. Hastings, A. D. Stone and H. U. Baranger, *Phys. Rev. B* **50** 8230 (1994). H.U. Baranger, R.A. Jalabert and A.D. Stone, *Phys. Rev. Lett.* **70** 3876 (1993).

<sup>30</sup> C. Gignoux, C. Berger, G. Fourcaudot, J.L. Grieco and H. Rakoto, *Europhys. Lett.* **39**, 171-176 (1997).

<sup>31</sup> R. Tamura, H. Sawada, K. Kimura and H. Ino, *Proceedings of the 6th International Conference on Quasicrystals*, Editors S. Takeuchi and T. Fujiwara, (World Scientific, Singapore 1998).

<sup>32</sup> N.P. Lalla, R.S. Tiwari and O.N. Srivastava, *J. Phys.: Condens. Matter* **7**, 2409 (1995).

Figure captions

Fig1 Chain  $N = 4$ : ABAA connected with perfect leads.

Fig2 Multifractal distribution of  $|s(N)|$  for the Fibonacci chain of 800 sites.

Fig3 Lyapunov exponents as a function of energy of a Fibonacci chain.

Fig4 Energy dependent phase diagram.

Fig5 Landauer resistance as a function of phason position  $x_P$ , for  $\varepsilon = 10^{-4}$ ,  $N = 35$  sites and  $m=1$ .

Fig6 Landauer resistances as a function of phason position  $x_P$  ( $N=2001, P=472$ ) for  $\varepsilon = [10^{-9}, 10^{-6}]$  and  $m=5$ . For higher values of  $\varepsilon$ , then  $\rho_N \rightarrow \infty$  which indicates that energy lies within a gap, or may be associated with a localized state.

Fig7 Power spectrum of the pattern given in the inset for  $m=5$  and same parameters as previous figure (bottom).

Fig8 Regular evolution of interference pattern for  $m = P, P + 1, P + 2$  and  $N = 2000, P = 472$ . For  $\varphi_s = P\pi/N$ , Fibonacci chain is always less resistive than the imperfect one whereas transition occurs for  $m = P + 1, P + 2, \dots$  dashed curves are the values for Fibonacci chains with same parameter  $m$  as imperfect one.

Fig9 Landauer resistance for values of scattering potential which unravel self-similar patterns as described in the text.

Fig10 Interferences pattern for several values of scattering potentials close to  $\varphi \sim \frac{\pi}{2}$ .

Fig11 Self similar interference pattern for  $N=3207, P=757$  and  $m=1605$ . Stability is ensured from  $\varepsilon = 10^{-3}$  down to the numerical resolution limit.

Fig12 Same as previous figure with different  $m$ .

Fig13. Landauer resistance interference pattern for  $\varepsilon = 0.5, N=2000$  and  $P=472$ .

